Numerical Analysis of Flow Characteristics in a Penstock Using COMSOL Multiphysics

Xalilov Bahromjon[1*], *Zayavitdinova* Nafisa[2], *Mirzayeva* Muhayyo[1], *Nazarova* Shokhida[3], *Bobojonova* Madina[1]

[1]Asia International University, Bukhara, Uzbekistan
[2]Bukhara state university. Bukhara, Uzbekistan
[3]Tashkent Institute of Irrigation and Agricultural Mechanization Engineers" National Research University Tashkent, Uzbekistan

Abstract. In this analysis, computational fluid dynamics (CFD) analysis of the penstock used in the hydropower plants was performed using the finite element method (FEM) by using COMSOL Multiphysics. The simulation is conducted in order to explore the differences in the flow behaviour, pressure distribution, and velocity profiles along the penstock geometry in the conditions of changing the inlet velocity (1 m/s, 2 m/s, 3 m/s, and 4 m/s). Turbulent Flow, k-epsilon interface is used whereby the trend of high Reynolds number flows are captured in case of hydropower conduits. Penstock model has features such as curvature and inclination to give them correspondences with real-life flow conditions. As demonstrated, variations in velocity gradients and dynamic pressure are much more considerable with appreciating inlet velocity, making it clear that robust structural design is required at greater flow rates. The zones of recirculation and secondary flow, especially close to bends, can be viewed using streamline visualizations that are vital in the evaluation of the loss of energy. The parametric study gives an understanding of how best to design the penstock in order to achieve better hydraulic performance and reliability of renewable systems.

1 Introduction

Hydropower represents a stable energy and renewable source of energy that contributes greatly towards electricity production at the global level [1]. The penstock is an important component of hydropower stations; it is a pressurized pipeline that delivers water between a reservoir or forebay and a turbine intake [2]. The hydraulic nature in penstocks has significant influence to the efficiency of energy, stability of pressure and stability of the system [3].

Lately, researchers paid attention to the numerical modelling of the penstock systems [4]. As computational fluid dynamics (CFD) techniques have improved, flow characteristics, pressure losses and the threat of cavitation and collapse due to loading can be analysed and evaluated under various operating conditions. Amongst the simulation software that one

* Corresponding author: bahromxalilov85@gmail.com

can work with is the COMSOL Multiphysics that is based on the finite element method (FEM) [5]. Here, it allows one to simulate both the flow of fluids and stress in the structural model [6].
A number of research papers analysed the fluid mechanics of penstocks by means of CFD. As an illustration, one could mention the research proposed by Xinran Guo et al. (2019) in which the authors investigate the fluctuation of power in hydropower stations employing the division of many turbines systems with central penstock. Based on CFD analysis, the authors demonstrate that the instability is primarily caused by pressure oscillations induced by vortices at the trifurcation based on CFD simulations with ANSYS. Among the structural improvement measures they assessed were the following. Installation of guide plate was an effective stabilization technique to power output. The research focuses on the importance of taking into account the dynamic flow stability in the design stage. It also proposes: an inlet-to-branch diameter ratio to reduce and outflow-flow velocities to insure better hydraulics [7]. In this way, the study of Yoga Satria Putra et al. (2022) explores the influence of penstock dimensions, namely diameter, slope and length, on the electrical power potential of a micro-hydro system with a CFD approach in Open FOAM. The authors conducted thirty simulations to examine flow behavior and energy loss in different penstock setups. The results indicate that a larger diameter and steeper slope can improve electric power output. However, longer penstocks generally lead to higher loss coefficients, which lowers performance. This study shows that CFD is an affordable tool for initial hydropower design and improvement [8].
Despite these advancements, detailed numerical studies on steady-state turbulent flow behavior in penstocks with multiple inlet velocities under the same geometric and boundary conditions are lacking. This gap is especially relevant for small- to medium-scale hydropower plants, where inlet velocity fluctuations often occur due to seasonal water availability and turbine regulation.
Therefore, this study aims to conduct a CFD analysis of water flow in a penstock using COMSOL Multiphysics. The analysis will apply four distinct inlet velocities: 1 m/s, 2 m/s, 3 m/s, and 4 m/s. The simulation will use the Turbulent Flow, k-ε interface, which is well-known for modeling high-Reynolds-number flows. The results will shed light on velocity distribution, pressure drop, and flow behavior under different inlet conditions. This work will contribute to design optimization and enhance the reliability of hydropower systems.

2 Materials and method

This study examines how different inlet velocities affect the internal flow behavior of a penstock system. We used numerical simulation in COMSOL Multiphysics for this research. The CFD module in COMSOL solved the governing equations of incompressible turbulent flow through a cylindrical penstock, which represents a micro-hydropower setup.

2.1 Geometry configuration

The penstock was modelled as a straight cylindrical pipe with a diameter of 400 mm (0.4 m) and a length of 7 m. This geometry replicates a common design in small-scale hydropower systems. The geometry was created within COMSOL using the built-in CAD tools.

2.2 Finite element solver

The computational domain was discretized using a free tetrahedral mesh, with refined elements near the pipe wall to resolve boundary layer effects accurately. A mesh independence test was conducted to ensure that the numerical results were not sensitive to mesh density. The final mesh was chosen to maintain a balance between computational cost and accuracy.

Table 1. Finite element solver

Elements type	Number of elements	Tetrahedra	Pyramids	Prisms
	80943	51925	386	28632

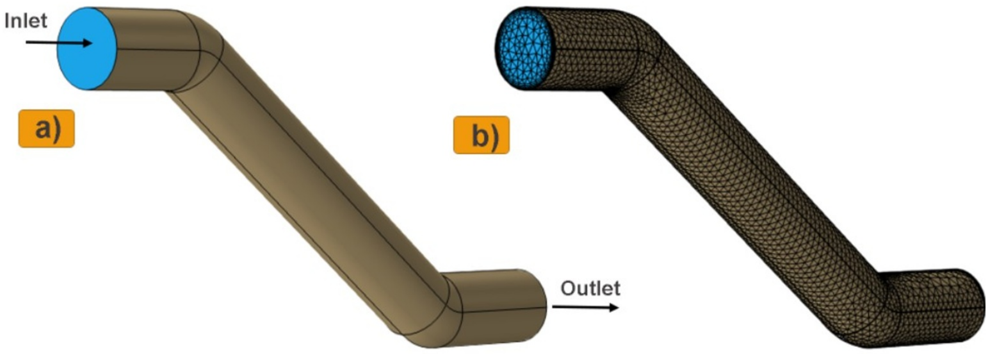

Fig. 1. a) Geometric view of penstock of hydropower systems, b) generated mesh size for penstock of hydropower systems

3 Equations and mathematics

The flow behavior in the micro hydroelectric turbine was modeled using the Reynolds-Averaged Navier–Stokes (RANS) equations combined with the standard k–ε turbulence model. These governing equations describe the conservation of mass and momentum for an incompressible turbulent fluid [9-11].

Continuity Equation:

$$\nabla \cdot \vec{u} = 0 \tag{1}$$

Where: $\vec{u}$ is velocity vector [m/s]

Momentum Equation:

$$\rho(\vec{u} \cdot \nabla)\vec{u} = -\nabla p + \nabla \cdot \left[\mu_{eff}\left(\nabla \vec{u} + (\nabla \vec{u})^T\right)\right] \tag{2}$$

Where: ρ-density of water [kg/m³], p- Pressure [Pa], μ_{eff}-effective dynamic viscosity [Pa·s].

Turbulent Viscosity:

$$\mu_{eff} = \mu + \mu_t \tag{3}$$

 https://doi.org/10.1051/e3sconf/202564803017

$$\mu_t = \rho C_\mu \frac{k^2}{\varepsilon} \tag{4}$$

Where: μ- Dynamic viscosity of water [Pa·s], μ_t-Turbulent viscosity [Pa·s], k-Turbulent kinetic energy [m²/s²], ε- Turbulent dissipation rate [m²/s³], C_μ-Empirical constant (= 0.09). Turbulence Model Equations (Standard k–ε).

$$\rho(\vec{u}\cdot\nabla)k = P_k - \rho\varepsilon + \nabla\cdot\left[(\mu) + \frac{\mu_t}{\sigma_k} ¿ \nabla k\right] \tag{5}$$

$$\rho(\vec{u}\cdot\nabla)\varepsilon = C_{1\varepsilon}\frac{\varepsilon}{k}P_k - C_{2\varepsilon}\frac{\varepsilon^2}{k} + \nabla\cdot\left[\left(\mu + \frac{\mu_t}{\sigma_\epsilon}\right)\nabla\varepsilon\right] \tag{6}$$

Where: P_k- Turbulent production term, $\sigma_k, \sigma_\epsilon$-Turbulent Prandtl numbers (= 1.0, 1.3), $C_{1\varepsilon}, C_{2\varepsilon}$-Model constants (= 1.44, 1.92)

4 Results and discussion

Figure 2 shows the distribution of velocity magnitude within a penstock at four different flow rates: 1 m³/s, 2 m³/s, 3 m³/s, and 4 m³/s. This simulation was done using COMSOL Multiphysics. The computational area represents a standard penstock design, including a bend to show realistic conditions. The velocity contours and streamlines use colour coding. The scale increases from blue for minimum velocity to red for maximum velocity, indicating how flow behavior varies across the penstock.

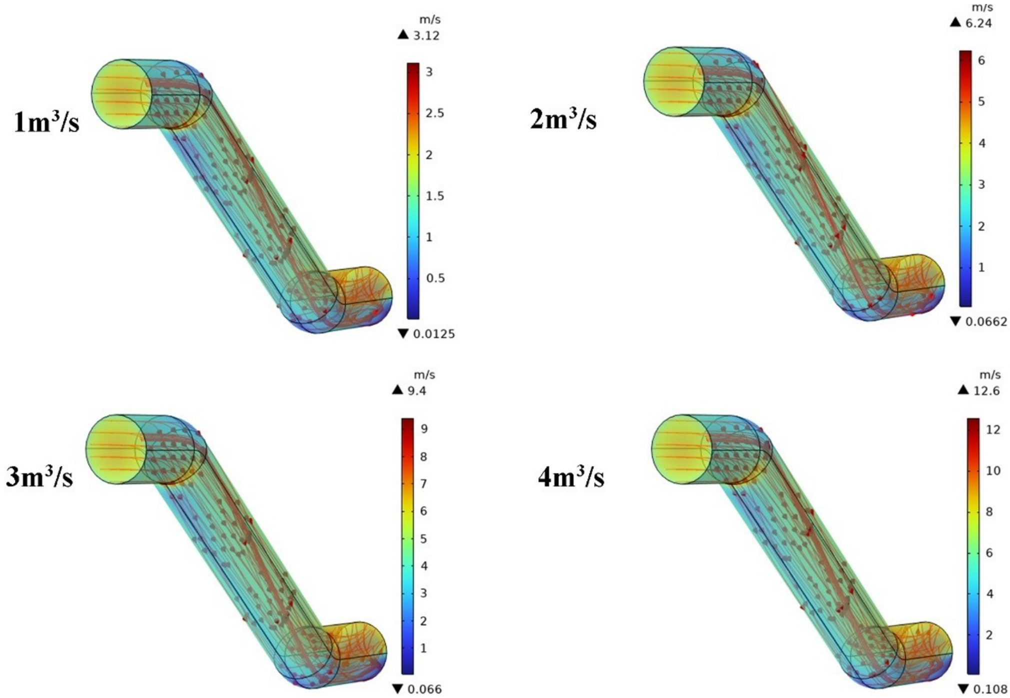

Fig. 2. Velocity magnitude of penstock of hydropower systems at four different flow rates

As expected, the velocity magnitude rises with the flow rate. Peak velocities are around 3.12 m/s, 6.24 m/s, 9.4 m/s, and 12.6 m/s for flow rates of 1 m³/s, 2 m³/s, 3 m³/s, and 4 m³/s, respectively. The streamline patterns show more flow acceleration along the inner walls and downstream of the bend, caused by momentum shift and secondary flow effects. Moreover, areas with lower velocity are found near the pipe walls, which aligns with boundary layer development. These findings highlight how flow rate affects internal velocity gradients and may impact hydraulic efficiency and structural stress in penstock systems.

Figure 3 shows the change in velocity magnitude along three different cross-sectional cut lines of the penstock: (a) at the inlet, (b) in the middle, and (c) at the outlet. These plots represent four different volumetric flow rates: 1 m³/s, 2 m³/s, 3 m³/s, and 4 m³/s. They illustrate how velocity changes along the internal arc length of the pipe.

In the inlet section (Figure 3a), the velocity profiles show a gradual increase in magnitude as the arc length increases. This trend is consistent for all flow rates and reflects the nature of developing flow, where the velocity boundary layer is still forming along the pipe wall. As expected, higher flow rates lead to much higher peak velocities. The profile becomes more curved with increasing flow rates.

In the middle section (Figure 3b), the velocity distribution becomes more balanced and reaches a relatively higher peak in the center. This suggests a shift toward fully developed flow. Here, the effects of inlet conditions lessen, and the flow stabilizes. Notably, at higher flow rates (3 m³/s and 4 m³/s), the velocity stays elevated over a wider central area, indicating a more uniform distribution of energy and momentum.

In the outlet section (Figure 3c), there is a slight drop in peak velocity, especially at the highest flow rates. The profiles appear more spread out, and the curvature is less steep. This may suggest energy loss, flow separation, or turbulence as the fluid leaves the penstock. The velocity drop near the ends of the arc length is more noticeable here, highlighting the effects of wall friction and potential three-dimensional flow in the outlet region.

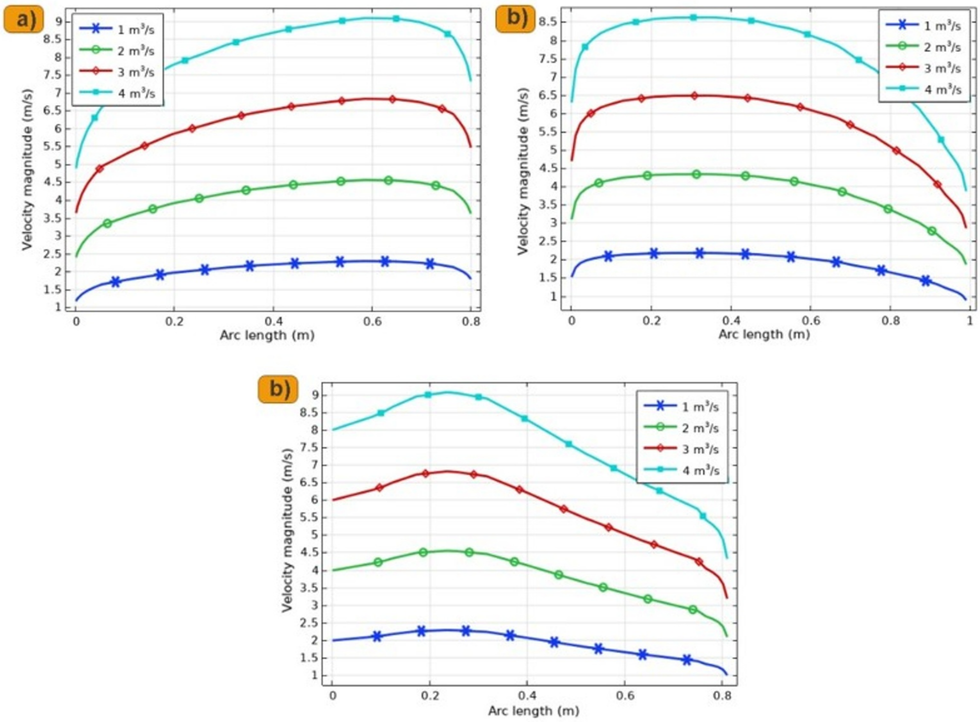

Fig. 3. Velocity variation of penstock of hydropower systems at three different Cut lines, a) Cut line at inlet section, b) Cut line at middle section, c) Cut line at outlet section.

Figure 4 shows the pressure distribution along three different cross-sectional lines of the penstock: (a) the inlet section, (b) the middle section, and (c) the outlet section. These distributions are examined for four different flow rates: 1 m³/s, 2 m³/s, 3 m³/s, and 4 m³/s. The pressure profiles are plotted against arc length for each section, allowing for a close look at pressure changes and flow behavior throughout the penstock. In the inlet section (Figure 4a), all flow rates show a noticeable pressure gradient. The highest pressures are near the start of the arc length. As the flow moves through the cross-section, the pressure gradually drops. This drop is more noticeable with higher flow rates, especially at 4 m³/s, where the pressure difference is the largest. This pattern makes sense, as higher flow speeds create more dynamic pressure loss near the inlet due to acceleration and entrance resistance. On the other hand, the middle section (Figure 4b) shows fairly consistent pressure distributions along the arc length.

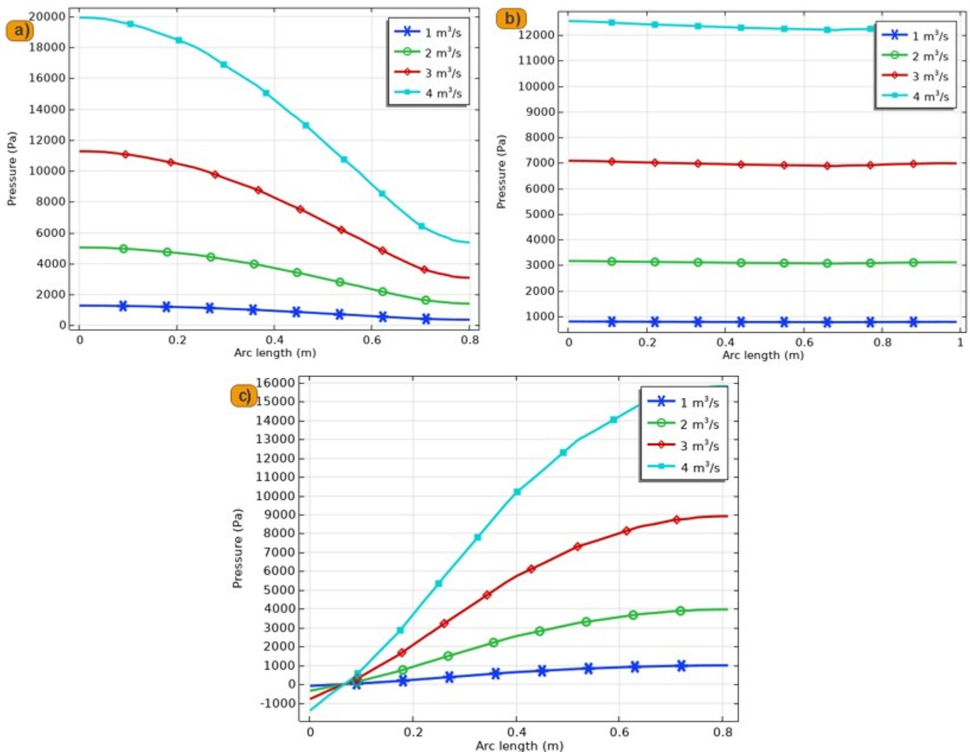

Fig. 4. Pressure variation of penstock of hydropower systems at three different Cut lines, a) Cut line at inlet section, b) Cut line at middle section, c) Cut line at outlet section.

This suggests a zone of stable flow, where pressure stays nearly the same across the section no matter the flow rate. This uniformity is usually linked to fully developed internal flow, where viscous and inertial forces balance out. In the outlet section (Figure 4c), the pressure distribution acts differently. Here, the pressure rises steadily along the arc length, especially at higher flow rates. The pressure gradient is steepest at 4 m^3/s, while lower flow rates have a gentler increase. This pattern likely results from flow slowing down and expanding as the fluid leaves the penstock, along with localized backpressure or changes in downstream conditions.

Conclusion

This study has demonstrated the effectiveness of computational fluid dynamics (CFD) employed through the use of finite element method (FEM) COMSOL Multiphysics. It measures the behavior of the turbulent flow in a penstock. Through alteration in the velocity of the entries, the study showed distinct trends in pressure and velocity profiles that are essential in design of hydropower systems. The findings indicate that larger the flow rate, the higher would be the dynamic pressures and steepness of velocities rates. All these may impose high structural loads on the penstock, particularly at curved and inclined sections.

Also, the streamline diagrams indicated that there was recirculation of flow around geometric changes, and secondary motions. Such phenomena lead to energy losses, which require superior attention in the course of design and maintenance planning. These flow complexities were well represented in the Turbulent Flow, k- e model making this model very helpful in high Reynolds-number hydrodynamic calculations.
The presented parametric analysis briefly provides the essential information regarding hydraulics of the penstocks. It forms a design and operating condition framework to help enhance efficiency, structural integrity and long-term reliability of renewable energy projects.

References

1. Luis Berga, The Role of Hydropower in Climate Change Mitigation and Adaptation: A Review, Engineering 2 (2016) 313–318. https://doi.org/10.1016/J.ENG.2016.03.004.
2. Ravi Kumar, S.K. Singal, Penstock material selection in small hydropower plants using MADM methods, Renewable and Sustainable Energy Reviews 52 (2015) 240–255. http://dx.doi.org/10.1016/j.rser.2015.07.018.
3. Ali Rezghi, Alireza Riasi, The interaction effect of hydraulic transient conditions of two parallel pump-turbine units in a pumped-storage power plant with considering "S-shaped" instability region: Numerical simulation, Renewable Energy 118 (2018) 896-908. https://doi.org/10.1016/j.renene.2017.11.067.
4. K.V. Alexandera, E.P. Giddens, Optimum penstocks for low head microhydro schemes, Renewable Energy 33 (2008) 507–519. https://doi.org/10.1016/j.renene.2007.01.009.
5. Rutuparna Ambekar, Nitesh Kumar, Shiva Kumar, H Girish, CFD analysis of cavitated flow in multi-groove water lubricated bearings with partial and full slip effects, Results in Engineering 27 (2025) 106693. https://doi.org/10.1016/j.rineng.2025.106693.
6. L. J. Yang, V.-J. Joseph, N.-K. Unnam, and B. Esakki, "Design and Numerical Simulation of Biomimetic Structures to Capture Particles in a Microchannel," Fluids, vol. 7, no. 1, p. 32, Jan. 2022, doi: 10.3390/fluids7010032.
7. X. Guo, H. Cheng, H. Wang, Y. Cheng, and M. Sun, "Analysis of the Power Fluctuations Caused by the Unstable Flow in the Trifurcation of Multi-Turbine Diversion Systems with Common Penstock in Hydropower Units," Energies, vol. 12, no. 15, p. 2941, Jul. 2019, doi: 10.3390/en12152941.
8. Y. S. Putra, E. Noviani, and M. Muhardi, "Numerical Study of The Effect of Penstock Dimensions on a Micro-hydro System using a Computational Fluid Dynamics Approach," Int. J. Renew. Energy Dev., vol. 11, no. 2, pp. 491–499, May 2022, doi: 10.14710/ijred.2022.42343.
9. C.D. Argyropoulos, N.C. Markatos, Recent advances on the numerical modelling of turbulent flows, Applied Mathematical Modelling 39 (2015) 693–732. http://dx.doi.org/10.1016/j.apm.2014.07.001.
10. F.H. Harlow, Fluid dynamics in Group T-3 Los Alamos National Laboratory (LA-UR-03-3852), Journal of Computational Physics 195 (2004) 414–433. http://doi.org/10.1016/j.jcp.2003.09.031.
11. H.W. Chiam, W.H. Azmi, N.M. Adam, M.K.A.M. Ariffin, Numerical study of nanofluid heat transfer for different tube geometries – A comprehensive review on performance, International Communications in Heat and Mass Transfer 86 (2017) 60–70. https://doi.org/10.1016/j.icheatmasstransfer.2017.05.019.